CENTRAL ASIAN JOURNAL OF SUSTAINABILITY AND CLIMATE RESEARCH (2023) 2(2):23-49

https://doi.org/10.29258/CAJSCR/2023-R1.v2-2/23-49.eng

Spatio-temporal patterns of different tree species response to climatic factors in south Kyrgyzstan

Maksim Kulikov [a], **Evgenii Shibkov** [a], **Erkin Isaev** [a], **Azamat Azarov** [a,b], **Roy Sidle** [a]

[a] University of Central Asia, 125/1 Toktogul Street, Bishkek, 720001, Kyrgyz Republic

[b] Czech University of Life Sciences Prague, Kamýcká 129, Praha, 165 00, Czech Republic

ABSTRACT

Understanding forest phenology is essential for monitoring global carbon budgets and managing vegetation resources in a changing climate. In southern Kyrgyzstan, walnut and wild apple trees dominate the forest landscape. These forests contain unique genetic diversity and offer potential for the development of climate-resilient crop varieties. They also support local communities through activities such as grazing, firewood collection, and fruit harvesting. However, these practices pose a threat to natural regeneration. Climate change exacerbates these challenges by altering their ecological niche. Despite this, few studies have examined forest phenology and its relationship to climate in Kyrgyzstan. To address this gap, we collected ecological data from forest plots in several protected areas and one forestry unit. This included tree species coordinates and landscape. Time series of vegetation indices, land surface temperature and precipitation were generated from remote sensing data. Regression analyses showed that temperature trends had limited predictive power for vegetation, while seasonal temperature variations had a positive effect on vegetation until excessive heat was reached, which had a negative effect. Precipitation trends and seasons had the most significant effects on vegetation, with lagged effects. Regression models were developed for Juglans regia L. (R^2=0.8) and Malus spp. (R^2=0.75) to predict vegetation index from temperature and precipitation data with high accuracy. Spatial heterogeneity in species response to climatic factors was evident within a small area. The study highlights the influence of landscape and climatic diversity on forest dynamics and emphasizes the importance of seasonal climate patterns over interannual trends.

ARTICLE HISTORY

Received: May 30, 2023
Accepted: Sept. 27, 2023
Published: October 10, 2023

KEYWORDS

forest, climate change, time series, remote sensing, species

CONTACT **Maksim Kulikov** maksim.s.kulikov@gmail.com, Mountain Societies Research Institute, University of Central Asia, 125/1 Toktogul Street, Bishkek, 720001, Kyrgyz Republic

Published by Kazakh German University, Almaty/Kazakhstan

1. Introduction

Kyrgyzstan occupies only 0.13% of Earth's land surface but has about 2% of the global flora and 3% of the faunal diversity (SAEPF et al., 2006). The walnut-fruit forests in the south of Kyrgyzstan represent a unique ecosystem with Juglans regia L. being the dominant tree species (Beer et al., 2008). They grow mainly on the western slopes of the Fergana Range and the southern slopes of the Chatkal Range in south Kyrgyzstan. This area is also the native home of many wild fruits and flowers with wide ranges of genetic diversity, including many widely cultivated plants like tulips (Botschantzeva & Varekamp, 1982; Zonneveld, 2009) and apples (Cornille et al., 2014).

The forests are dominated by Juglans regia L. and represent one of the most important genetic pools for this species and a primary source for new varieties (Beer et al., 2008; Molnar, 2011; Spengler, 2019; Torokeldiev et al., 2019; Vinceti et al., 2022). The apple trees and their patches are sporadically distributed in the walnut forest (Wilson et al., 2019). Some trees have natural origin, whereas others are artificially planted mainly by forestry units. The most numerous wild apple species are Malus sieversii (Ledeb.) M. Roem. and Malus kirghisorum Al. Fed. & Fed., with red apple Malus niedzwetzkyana Dieck being far less numerous (~ < 10% of the apple population).

These areas are also some of the most populated places in Kyrgyzstan, with many people dependent on natural resources for their income. Large villages are located near or within nature-protected areas. Kara-Alma village is very close to the Kara-Alma forestry unit where the primary income sources are walnut collection, animal husbandry, and wild apple collection (Azarov et al., 2022). Villages of Arslanbob, Gumkhana, and Kyzyl-Unkur are located around Dashman Nature Reserve, where the main pressures are walnut collection, animal husbandry, and tourism. Walnut collection, animal husbandry, tourism, and beekeeping are the primary income sources in the villages of Arkyt in in the middle of Sary-Chelek Biosphere Reserve and Kashka-Suu near the Padysha-Ata Nature Reserve (Azarov et al., 2022).

Walnut harvesting provides substantial income to local communities (Azarov et al., 2022; Borchardt et al., 2010; Shigaeva et al., 2018). Thus, the forest is a vital community resource. Nevertheless, the value of ecosystem services of these forests still needs to be evaluated. Due to the high importance of the forest, human impact is the main threat to these ecosystems, as the collection of walnuts and wild apples limits their natural regeneration capacity (Cantarello et al., 2014; Orozumbekov et al., 2014). Grazing in the forests also poses a significant threat to the trees and the ecosystem. Animals destroy grass and walnut seedlings, which leads to forest aging (Borchardt et al., 2010) and soil erosion due to compaction and subsequent concentrated runoff (Borchardt et al., 2013; Kulikov et al., 2017).

Gathering wild apples is an important source of income for local communities (Azarov et al., 2022; Shigaeva et al., 2007). Other tree species grow in these forests but do not develop forested patches and are distributed sporadically within the walnut and apple forests. These species include Acer turkestanicum Pax, Pyrus turcomanica Maleev, Prunus Sogdiana Vassilcz., Crataegus spp., Betula spp., Juniperus spp., Populus spp., Fraxinus spp., Lonicera spp., Berberis spp., Cotoneaster spp., Rosa spp., and other species. The forests are characterized by significant spatial variability in species and density due to complex orography (Figure 1).

Figure 1. Sary-Chelek Biosphere Reserve.

Walnut-fruit forests are particularly susceptible to climatic factors (Winter et al., 2009) as are other forests in Kyrgyzstan (Isaev, Ermanova, et al., 2022). Broader regional studies indicate that tree growth and tree line elevation are being affected by climate change in Mongolia (Dulamsuren et al., 2013, 2014) and in eastern Tibetan Plateau (Wang et al., 2019). Thus, climate change is another factor affecting these forests, exacerbated by their immobility and low adaptive capacity. However, Schickhoff et al. (2015) did not find a significant shift in the Himalayan treeline due to climate change, and a review of forest responses to climate change (Shaw et al., 2022) suggests large regional variability in climate response. At the same time, there are few ecological studies of forest ecosystems in Central Asia, suggesting that more research is needed to elucidate the response of forests to climate change (Wilson et al., 2021). Vegetation phenology indicates the annual development of plants and is an excellent variable for understanding of vegetation dependencies on climatic factors, with possible implications for climate change. At the same time, the development

of remote sensing and vegetation indices provide long and spatially explicit time-series for approximation of vegetation phenology. There have been several phenological studies in Kyrgyzstan and the region (Henebry et al., 2017; Kulikov & Schickhoff, 2017; C. Li et al., 2021; Tomaszewska et al., 2020; Tomaszewska & Henebry, 2020) using remotely-sensed vegetation indices and mainly dealing with grasslands.

Tomaszewska et al. (2020) found significant correlations between snow seasonality and vegetation peaks approximated by normalized difference vegetation index (NDVI) with warmer spring temperatures and less snow, leading to lower pasture productivity in Naryn province, Kyrgyzstan. Tomaszewska & Henebry (2020) noted that 55 to 70% of the variation in the vegetation phenological metric (accumulated growing degree-days) can be explained by elevation and snow cover metrics, making precipitation and terrain factors the main covariates for vegetation phenology in Naryn and Alai regions of Kyrgyzstan. Wu et al. (2023) found that extreme climate events have a significant impact on land surface phenology, indicating a delay in the onset of the growing season and an advance in the end of the growing season, and thus a general shortening of the growing season in Central Asia. However, the area of walnut-fruit forests in south Kyrgyzstan indicates growing season increases (0.5 – 1 day yr-1) in contrast to most of Central Asia (Wu et al., 2023). On the other hand, Li et al. (2021) distinguished between different vegetation types and found distinct spatial heterogeneity for different vegetation, indicating that they should be analyzed separately and that spatial discretization is important to avoid mixing of different meaningful phenological signals. They also showed that there is a significant relationship between the phenology of vegetation and temperature in Xinjiang, China. Kulikov & Schickhoff (2017) conducted spatial discretization of the entire area of Kyrgyzstan based on the temporal behavior of remotely sensed vegetation indices and climatic factors, which indicated significant spatial heterogeneity depending on the vegetation classes and orography. These studies demonstrate the importance of granular and meaningful spatial discretization of remotely sensed indices and climatic factors, especially in highly diverse mountain environments, to understand better how different vegetation communities and species respond to climatic variables.

Most vegetation biodiversity studies in walnut-fruit forests assess the current (i.e., static) spatial distribution of species in the forests (Borchardt et al., 2010; Cantarello et al., 2014; Orozumbekov et al., 2014; Wilson et al., 2019). These studies outline the contemporary use of forests, species distribution, and their covariates. Pollen and stomata studies (Beer et al., 2007, 2008; Beer & Tinner, 2008) explore the history of forests and attempt to reconstruct past species composition to aid in reconstructing climate history. Other studies examine tree-ring patterns and their relation to climatic factors and mass movement events (Isaev, Ermanova, et al., 2022; Kang et al., 2022; Winter et al., 2009; Zaginaev et al., 2016, 2019) confirming that tree rings are suitable covariates for restoration of missing climate data. Broader studies of Central Asian vegetation phenology (Gessner

et al., 2013; Kariyeva et al., 2012; Propastin et al., 2007, 2008b) used metrics such as season onset, end, and peak derived from remotely sensed vegetation indices with accumulated precipitation and temperature indices for linear regression analysis to identify relationships between vegetation and climatic variables. These investigations also revealed significant covariation of climatic and vegetation metrics with different temporal lags in diverse vegetation. However, these studies did not use many time-series decomposition and analysis methods that could reveal more interactions and patterns (Kulikov & Schickhoff, 2017). Different time series feature engineering approaches such as time series decomposition, lag and window features, and nonlinear transformation of predictors can reveal more complex relationships between forest vegetation and climatic parameters.

Central Asian grasslands contribute significantly to carbon sequestration, a significant control on climate change, including increases in CO_2, temperature, and precipitation (Fang et al., 2019; Li et al., 2013; Zhu et al., 2019). Forests, which are far less abundant than grasslands in Central Asia, are also important carbon sinks and require investigation and proper management to benefit from their carbon sequestration capacity (Li et al., 2013). However, few studies have been conducted in Kyrgyzstan on the phenology of forest vegetation and the phenology of different forest types. Similarly, little attention has been paid to quantifying the effects of climate on trees and modeling these interactions. Here, we address this research gap by identifying phenological patterns of different forest types and tree species and their temporal relation with climatic factors like land surface temperature and precipitation. We then quantify these relations by developing regression models to investigate the resilience of walnut-fruit forests to climate change.

2. Methods

2.1. Study area

The study area includes walnut-fruit forests on the western slopes of the Fergana Range and the southern slopes of the Chatkal Range (Figure 2). These are in the Padysha-Ata Nature Reserve, Sary-Chelek Biosphere Reserve, Dashman Nature Reserve, and Kara-Alma forestry unit in the Jalal-Abad province in south Kyrgyzstan (Table I). These areas are some of the most populated places in Kyrgyzstan. We selected them because they represent the main forest ecosystems in the region, contain large areas of habitat for the chosen species, and encompass the most significant population of these tree species.

Different opinions have emerged on whether M. niedzwetzkyana Dieck and M. kirghisorum Al. Fed. & Fed. are subspecies of M. sieversii (Ledeb.) M. Roem. (van Nocker et al., 2012; Volk et al., 2013). This issue requires additional genetic research to clarify species assignment, as well as a common understanding of species ‘boundaries’ (Mace,

2004). We decide to recognize M. niedzwetzkyana Dieck as a separate species and M. kirghisorum Al. Fed. & Fed. as a subspecies of M. sieversii (Ledeb.) M. Roem as proposed by the Red Data Book of the Kyrgyz Republic (SAEPF et al., 2006) and the IUCN Global Red List (IUCN, 2022). M. niedzwetzkyana Dieck is rated as 'Vulnerable' in the national Red Data Book and 'Endangered' by the IUCN Global Red List, M. sieversii (Ledeb.); M. Roem. is 'Least Concern' and 'Vulnerable' respectively in the two lists. M. sieversii (Ledeb.) M. Roem. is considered an ancestor of M. orientalis Uglitzk. and M. domestica (Suckow) Borkh. is a domestic variety of apple trees (Cornille et al., 2014). These wild ancestors of domestic apple species are of great value per se for their high anthocyanin content(van Nocker et al., 2012; Wang et al., 2015) and as a genetic pool for new cultivars (Cornille et al., 2014; Yan et al., 2008).

The forests occupy the foothills of the Fergana and Chatkal mountain ranges at altitudes from 1000 to 2000 meters above sea level. The terrain consists of gently rolling hills and mountains with exposed rock; sandstone and limestone are the dominant parent materials for soil development (Adyshev et al., 1987). Soils on rocky slopes are represented by Cambisols, Umbrisols, and Leptosols (IUSS Working Group WRB, 2006), which consist mainly of silt and fine sand (Kulikov et al., 2017) with a high potential for water erosion. These areas receive high annual precipitation reaching 900 – 1050 mm (Aitaliev et al., 2020). The long-term mean air temperature in January is between -2°C and -11°C; the mean air temperature in July is between 23°C and 27°C (Aitaliev et al., 2020).

Table I. Description of the study sites.

Name	Coordinates	Area km^2	Description
Sary-Chelek Biosphere Reserve	E71.933132° N41.868115°	237.96	Sary-Chelek is a UNESCO biosphere reserve on the south slope of the Chatkal Range in south Kyrgyzstan
Padysha-Ata Nature Reserve	E71.683163° N41.717878°	680.55	Padysha-Ata Nature Reserve on the south slope of the Chatkal Range
Dashman Nature Reserve	E73.02838° N41.37059°	79.36	Dashman Nature Reserve has one of the largest walnut populations in Kyrgyzstan on the western slope of the Fergana Range
Kara-Alma forestry unit	E73.341518° N41.249517°	267.6	Kara-Alma forestry unit has the largest population of wild apple trees on the western slope of the Fergana Range

The forests consist mainly of Juglans regia L. trees with Malus sieversii (Ledeb.) M. Roem., M. niedzwetzkyana Dieck, Pyrus korshinskyi Litv., Acer turkestanicum Pax,

Pyrus turcomanica Maleev, Prunus Sogdiana Vassilcz., Picea schrenkiana Fisch. & C.A. Mey., Crataegus spp., Betula spp., Juniperus spp., Populus spp., Fraxinus spp., Lonicera spp., Berberis spp., Cotoneaster spp., Rosa spp., and other species (Lazkov & Sultanova, 2011). Grasses are mainly represented by Festuca rupicola Heuff., Dactylis glomerata L., Bromus tectorum L., Trifolium repens L., Trifolium pratense L., Poa pratensis L., Koenigia coriaria (Grig.) T.M.Schust & Reveal, Malva neglecta Wallr, Eremurus fuscus (O. Fedtsch.) Vved., Taraxacum officinale F.H. Wigg., Geum urbanum L., Impatiens parviflora DC., Brachypodium sylvaticum (Huds.) P. Beauv., Ligularia thomsonii (C.B. Clarke) Pojark., Ranunculus polyanthemos L., Vicia tenuifolia Roth, and Hypericum perforatum L. (Borchardt et al., 2010; Lazkov & Sultanova, 2011).

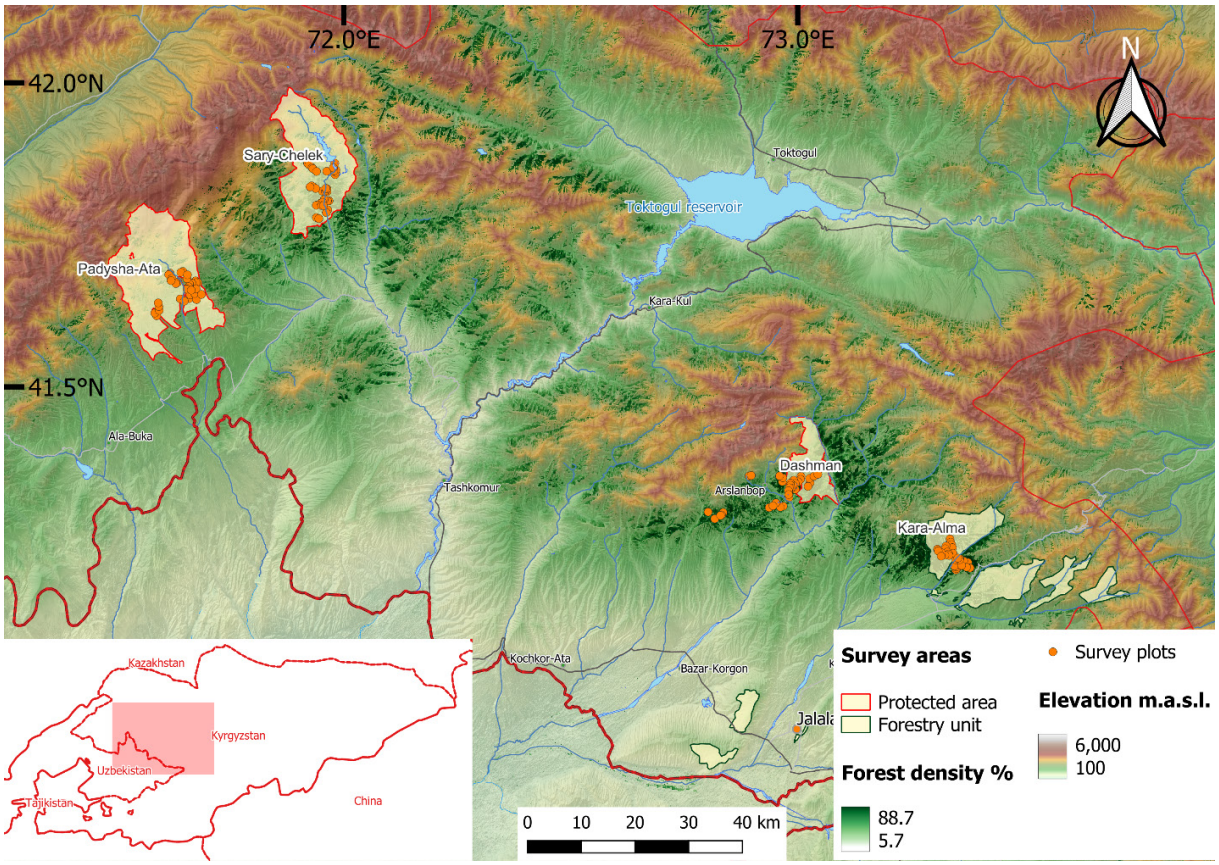

Figure 2. Research area. (Sources: elevation data from USGS, roads, settlements, and water bodies from OpenStreetMap, forest cover from Global Forest Watch). A total of 133 survey plots, Kara-Alma - 32, Dashman - 35, Padysha-Ata - 32, Sary-Chelek - 34.

2.2. Field data collection

Field data were collected during the summers of 2021 and 2022. In total, environmental data were collected from 133 plots across the four study sites (Kara-Alma - 32, Dashman - 35, Padysha-Ata - 32, Sary-Chelek - 34), including GPS coordinates of

1428 trees (by species) on those plots. Plots were selected using a stratified random sampling approach. Prior to the field trip, we divided the study areas into strata of different elevation, slope, and aspect to cover the full variability of geographic features that influence vegetation distribution. In the field, we selected plots that were most representative of the surrounding forest and stratum, excluding areas with unrepresentative human impacts such as livestock congregation areas, huts, and roads. However, some plots at the base of slopes included roads or trails because there is almost always a road or trail at the bottom of a side valley or at the top of a side ridge.

The plots selected for the description of environmental characteristics were 100 x 100 m in size. These included slope gradient in 3 categories (0-15°, 15-30°, 30-45°), aspect, slope shape (convex, concave, straight), position on the slope (top, middle, bottom), and land cover class (Figure 2). The coordinates of all plots were recorded by GPS as stem coordinates of a sample of 10-15 trees from the plot, noting their species, circumference at breast height, and presence of flowers or fruits. The trees measured were representative of the forest stand in the plot; these were the dominant species, and their proportion was maintained in the sample to represent the species composition of the forest in the plot. However, only Juglans regia L. and Malus spp. were used in the analysis, as they were the most abundant species with the highest representation in our data set; they were present in all study sites and could be used for comparative analysis.

2.3. Preparation of raster data

The data analysis was conducted in Google Colab using Python 3.10.12 and involving Google Earth Engine Python API for the remotely sensed data manipulations.

NDVI and EVI have a long history of use as vegetation covariates in remote sensing research because live and healthy vegetation reflects more in the near-infrared spectrum and less in the red spectrum. Thus, by applying Equation (1), we can calculate a variable that will by design take values around 0, where anything less than 0 means “no vegetation” and anything greater than 0 means green vegetation. Several studies also indicate that EVI is a good covariate for biomass and carbon stocks, improving estimation models in different ecosystems (Dai et al., 2020; Eckert, 2012; Gao et al., 2000; Huete et al., 2002; Jiang et al., 2021; Rahman et al., 2005; Xiao et al., 2019; Zhang et al., 2016), which may not be the case for boreal forests (Loranty et al., 2018).

$$EVI = G * \frac{(NIR - Red)}{(NIR + C_1 * Red - C_2 * Blue + L)} \quad (1)$$

where:

EVI – enhanced vegetation index,

NIR – near-infrared reflectance,

Red – red reflectance,

Blue – blue reflectance,

L – vegetation background correcting coefficient, L = 1,

C_1, C_2 – aerosol correction coefficients, C_1 = 6, C_2 = 7.5,

G – empirical correcting factor, G = 2.5.

We chose EVI because it is more applicable to our forest conditions, as EVI corrects for some atmospheric conditions and canopy background noise and is more sensitive in areas with dense vegetation. Equation (1) incorporates the correction values L, C_1, and C_2, and uses the blue band in contrast to the NDVI equation. These enhancements allow the index to be calculated as a ratio between the R and NIR values, while reducing background noise, atmospheric noise, and saturation in most cases (Landsat Enhanced Vegetation Index | U.S. Geological Survey, n.d.). Thus, using EVI instead of NDVI helps to reduce the noise and increase the signal from the canopy.

We used Sentinel-2 data (product 'COPERNICUS/S2' in Google Earth Engine) as the main remotely sensed data source for the calculation of vegetation indices for the period 2016 - 2022. Sentinel-2 offers a high spatial resolution of 10 m and a frequent revisit rate of 5 days (User Guides - Sentinel-2 MSI - Sentinel Online - Sentinel Online, 2023). Although the Landsat mission has a longer history of surface observations and a large dataset of satellite imagery, its spatial resolution of 30 m is much coarser than the average canopy area. Therefore, Sentinel-2 imagery was selected to capture the vegetation signal with greater precision. All images were cloud-masked using the supplied cloud mask. The values of all spectral bands were divided by 10,000 because they are scaled by 10,000. Next, the EVI was calculated using Equation (1) in Google Earth Engine.

The EVI images were then combined into monthly vegetation grids for each month between 2016 and 2022, taking the maximum value of the pixels. We superimposed all images taken within a month and took the maximum value of each superimposed pixel to create the image representing the entire month. By taking the maximum value of all pixels within a month, we further cleaned up aerosol and haze effects (which typically reduce vegetation indices) and ensured data consistency. Thus, we obtained a monthly time series of rasters of vegetation indices for our study areas.

To approximate the temperature in our study area, we used Landsat 7 and Landsat 8 datasets with precalculated land surface temperature (LST), products of 'LANDSAT/LE07/C02/T1_L2' and 'LANDSAT/LC08/C02/T1_L2' from Google Earth Engine, respectively. The time period considered was the same as that of the

Sentinel-2 images (i.e., 2016 - 2022). These images were also masked for clouds and cloud shadows using the provided mask, and the values were recalculated from Kelvin to degrees Celsius. They were then combined into monthly rasters using the maximum function to eliminate any possible effect of aerosols, as described for EVI. This resulted in monthly time series of LST raster images.

The precipitation data used in this study were provided by the Climate Hazards Group InfraRed Precipitation with Station data (CHIRPS), namely the 'UCSB-CHG/CHIRPS/DAILY' product of Google Earth Engine. These are ready-to-use daily rasters that have been recalculated to monthly precipitation values. We preferred this dataset over others because it provides more than 30 years of quasi-global precipitation data based on 0.05° resolution satellite imagery and local station data.

We selected data from different sources for the vegetation indices, LST and precipitation to avoid co-variation inherited from the same initial data source. The main parameter in selecting the datasets was high spatial resolution to best quantify canopy heterogeneity. The dataset should have at least monthly temporal resolution to capture phenological changes in vegetation.

2.4. Preparation of time-series

Monthly values of vegetation indices, LST, and precipitation were attributed to each tree based on its coordinates. Using the tree coordinates, we assigned mean values of all pixels within a 10 m radius buffer around each tree. Thus, we obtained a monthly time series of vegetation index (EVI), LST, and precipitation as spatial means for each measured tree.

There were some missing values at some locations and months, mainly due to cloud masking or missing values on Landsat 7 imagery due to scanline errors. Missing values were replaced by smoothing with weighted averages of the previous and following months and the same month for the previous and following 3 years, with values closer in time to the missing value given higher weights. This approach ensures intra- and inter-annual data consistency. The following equation details the approach used to replace the missing values.

$$V_t = \frac{a * V_{t\pm36} + b * V_{t\pm24} + c * V_{t\pm12} + d * V_{t\pm1}}{2 * (a + b + c + d)} \quad (2)$$

where:

V_t – missing value (weighted mean) at time t,

$V_{t\pm n}$ – existing value at time t + n and t - n (in months), if some of these values were also missing, they were omitted, and the denominator changed accordingly,

a, b, c, d – weights for the variables, we used values 1, 2, 3, 4 respectively.

2.5. Regression analysis

All time series of predictors (i.e., climatic factors) were decomposed into additive seasonal and trend components using the "statsmodels.tsa.seasonal.seasonal_decompose" package (Statsmodels.Tsa.Seasonal.Seasonal_decompose — Statsmodels, 2023) in Python 3.10.12 (Google Colab). This provided time series of trends and seasonal components for each climatic factor (LST and precipitation). Then, we performed regression analysis using OLS (ordinary least squares) to predict EVI from trends and seasonal components of LST and precipitation. Temperature may promote EVI in spring with a positive correlation and depress EVI in summer heat with a negative correlation. We applied a threshold to divide the seasonal component of LST into two parts to evaluate temperature promoting and depressing variables separately by specifying values below and above a certain threshold. We tried several options for this temperature threshold between 8 and 11°C, as well as no separation, to obtain the best fit of the linear regression equation. Equations (3, 4) outline the splitting function we used.

$$TS^{shoe} = \begin{cases} TS, & TS \leq T_{th} \\ T_{th}, & TS > T_{th} \end{cases} \quad (3)$$

$$TS^{hat} = TS - TS^{shoe} \quad (4)$$

where:

TS – LST seasonal component (Temperature Seasonal),

T_{th} – LST threshold, taking values of 8 – 11°C,

TS^{shoe} – first part of LST seasonal component with values below the threshold,

TS^{hat} – second part of LST seasonal component with values above the threshold.

Since the response of the EVI to different climatic factors can take several months, we also applied different time lags of 0-4 months for seasonal components and 0-12 months for trend components. The coefficient of determination (R^2) was the main metric used to fit the model and the p-value was the main metric used to select the predictors. Regression analysis was performed separately for Malus spp. and Juglans regia L. using all data from all study sites. Equation (5) outlines our regression approach.

$$EVI_t = a * TS^{shoe}_{t+w} + b * TS^{hat}_{t+w} + c * TT_{t+x} + d * PS_{t+y} + g * PT_{t+z} + e \quad (5)$$

where:

EVI_t – Enhanced Vegetation Index at time t,

TS^{shoe} – first part of LST seasonal component with values below the threshold,

TS^{hat} – second part of LST seasonal component with values above the threshold,
TT – LST trend component (Temperature Trend),
PS – precipitation seasonal component (Precipitation Seasonal),
PT – precipitation trend component (Precipitation Trend),
a, b, c, d, g – regression coefficients,
w, x, y, z – temporal shifts in months (lags),
e – error.

We tested all possible combinations of predictor lag shifts and LST seasonal component partitioning thresholds to find the optimal linear model. For model fitting, negative lags were not used to avoid artificial overfitting, as EVI is not expected to respond to future changes in LST or precipitation. The lag shifts for TSshoe and TShat within each combination were always the same, as this is a single time series split into two parts. We also did not use lags greater than 4 months for seasonal components and greater than 12 months for trend components because we do not believe that climatic factors can have a meaningful impact on EVI beyond these periods (Gessner et al., 2013; Klein et al., 2012; Propastin et al., 2007, 2008b, 2008a), but the covariation could be attributed to annual cycles. Both predictors, LST and precipitation, had data before 2016, so we used the real data after shifts. We used OLS linear regression package "statsmodels.regression.linear_model.OLS" (Statsmodels.Regression.Linear_model.OLS - Statsmodels 0.15.0 (+59), n.d.) in Python 3.10.12 (Google Colab).

The main reason for choosing OLS was to reveal interactions between vegetation and climatic parameters. We used intensive feature engineering such as season and trend decomposition, nonlinear transformations, and lagging to explore the complexity of the relationships more deeply. We chose not to use more advanced time series forecasting techniques and machine learning approaches, even though they might provide better predictive power but with a poorer understanding of the model.

2.6. Comparison with t-test

We used t-test with equal variance to test for meaningful differences of EVI between different sites and different species by months. T-test was done with "statsmodels.stats.weightstats.ttest_ind" package (Statsmodels.Stats.Weightstats. Ttest_ind - Statsmodels 0.14.0, n.d.) in Python 3.10.12 (Google Colab). Monthly EVI for Juglans regia L. and Malus spp. were compared to identify meaningful differences between study sites. We also used t-tests to identify meaningful differences between Juglans regia L. and Malus spp. in the same study sites. These were conducted to determine whether differences in monthly EVI values between species and sites were meaningful.

3. Results

3.1. Data overview

The lowest monthly mean precipitation is in Padysha-Ata - 20.03 mm month-1, the highest level is in Dashman - 39.35 mm month-1, followed by Sary-Chelek and Kara-Alma - 35.67 and 33.72 mm month-1, respectively (Figure 3a). The highest monthly mean land surface temperature was in Dashman (18.0°C), the lowest in Padysha-Ata (15.9°C), followed by Kara-Alma and Sary-Chelek (16.2 and 17.1°C, respectively) (Figure 3b). The mean elevations of the plots were 1824 m.a.s.l. in Padysha-Ata, 1614 m.a.s.l. in Dashman, 1518 m.a.s.l. in Sary-Chelek, and 1585 m.a.s.l. in Kara-Alma (Figure 3c). Sary-Chelek had significantly greater variability in plot elevations (Figure 3c). The mean slope gradients of the study plots were as follows: Padysha-Ata - 24.8°, Sary-Chelek and Kara-Alma - 16.7°, and Dashman - 15.2° (Figure 3d). Dashman had the highest land surface temperature and precipitation (Figures 3a, b), and Padysha-Ata had the highest elevation and steepest plots (Figures 3c, d). Kara-Alma was an average study site with intermediate values for all variables.

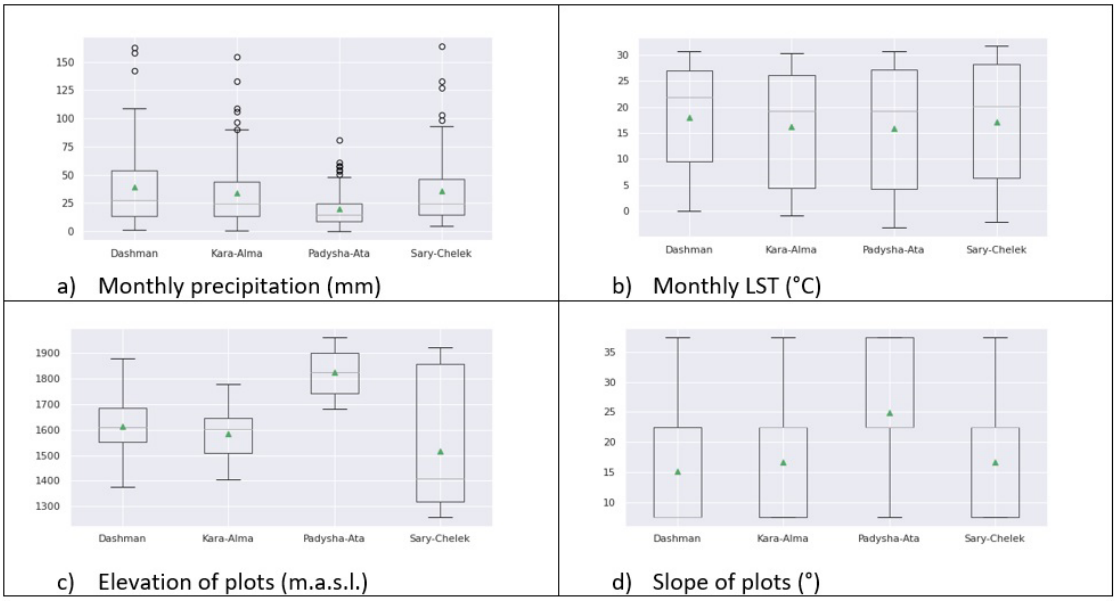

Figure 3. precipitation, LST, elevation and slope of plots for the 4 study sites. The box edges extend from Q1 to Q3 with a line at the median and green triangle at mean. Whiskers show the range of data but not greater than 1.5*(Q3-Q1).

Despite the sampling approach in which we tried to randomly sample different environmental conditions, the distribution of these conditions in plots differed among the various study areas due to different natural conditions. Overall, the monthly mean EVI values show a similar pattern in all sites, with low values in winter and fall, a rapid increase in April, and the highest values in June, followed by a slow decrease

(Figure 4). However, the monthly pattern of EVI values is similar between Dashman and Kara-Alma and between Padysha-Ata and Sary-Chelek, but somewhat different between these two groups. In particular, spring EVI values at Dashman and Kara-Alma increase rapidly in April with high interannual variability, while slower growth occurred in April and May at Padysha-Ata and Sary-Chelek. The November-March EVI values at Dashman and Kara-Alma are also significantly lower than those at Padysha-Ata and Sary-Chelek (Figure 4).

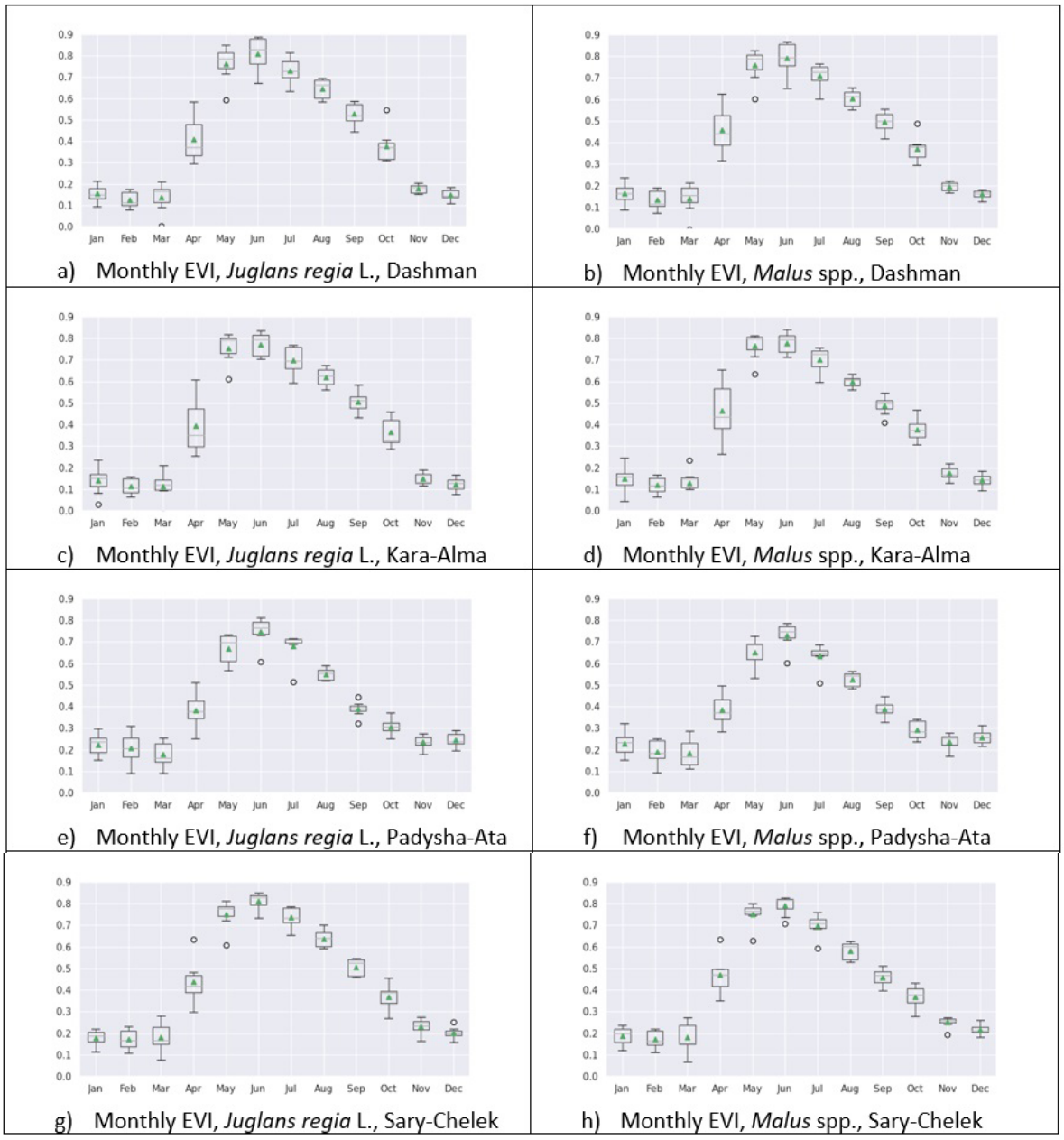

Figure 4. Monthly distribution of EVI for 2016 – 2022 by study sites and species. The box edges extend from Q1 to Q3 with a line at the medianand green triangle at mean. Whiskers show the rangeof databut not greater than 1.5*(Q3-Q1).

3.2. Comparison of sites and species with t-test

Comparing the same species among the study sites for both Juglans regia L. and Malus spp., all EVI values for the vegetation period (April - October) in Padysha-Ata are significantly lower than those in other study sites ($p < 0.05$) (Figure 4). Sary-Chelek had significantly lower EVI than Dashman for Juglans regia L. in April, May, and September, and for Malus spp. from July to September. EVI values in Sary-Chelek were significantly higher than in Kara-Alma in April and June to August for Juglans regia L., and significantly lower in August and September for Malus spp. Dashman had significantly higher EVI values than Kara-Alma for Malus spp. in June and July, and for Juglans regia L. in April to October (Figure 4).

Comparing species in the same study sites, EVI values in Padysha-Ata were significantly lower for Malus spp. than for Juglans regia L. in July and August ($p < 0.05$). In Sary-Chelek, EVI values for Malus spp. were significantly lower than for Juglans regia L. in June to September. In Dashman, EVI values for Malus spp. were significantly lower than those for Juglans regia L. in June through September, while in Kara-Alma, EVI values in August and September were significantly lower for Malus spp. Overall, EVI values for Malus spp. were generally lower than those for Juglans regia L. in all study sites in mid and late summer.

3.3. Time series seasonal and trend decomposition

The seasonal components of LST are similar among the study sites, with the lowest values in winter, followed by a gradual increase and a maximum in August (Figures 5a, c, e, g - red line). However, the fluctuations of the temperature trend components in Dashman are similar to those in Kara-Alma, but with different means (Figures 5b, d - red line), and the trend in Padysha-Ata is similar to that in Sary-Chelek, but with different means (Figures 5f, h - red line). The LST trends in Dashman and Kara-Alma are different from those in Padysha-Ata and Sary-Chelek. The temperature trend curve does not follow any of the EVI trend curves in the study areas (Figures 5b, d, f, h), and their maximum correlation coefficients were only 0.009 - 0.02 at lag 4, whereas the correlation coefficient of the seasonal components of temperature with EVI reached r values of 0.77 - 0.87 at lag 0, depending on the species and study area.

The seasonal distribution of precipitation was very different among the study sites (Figures 5a, c, e, g). Dashman has a peak in April with another in October-November (Figure 5a), similar to Kara-Alma (Figure 5c) and Sary-Chelek with the first peak in May (Figure 5g). Padysha-Ata had smaller peaks in February and October-November (Figure 5e).

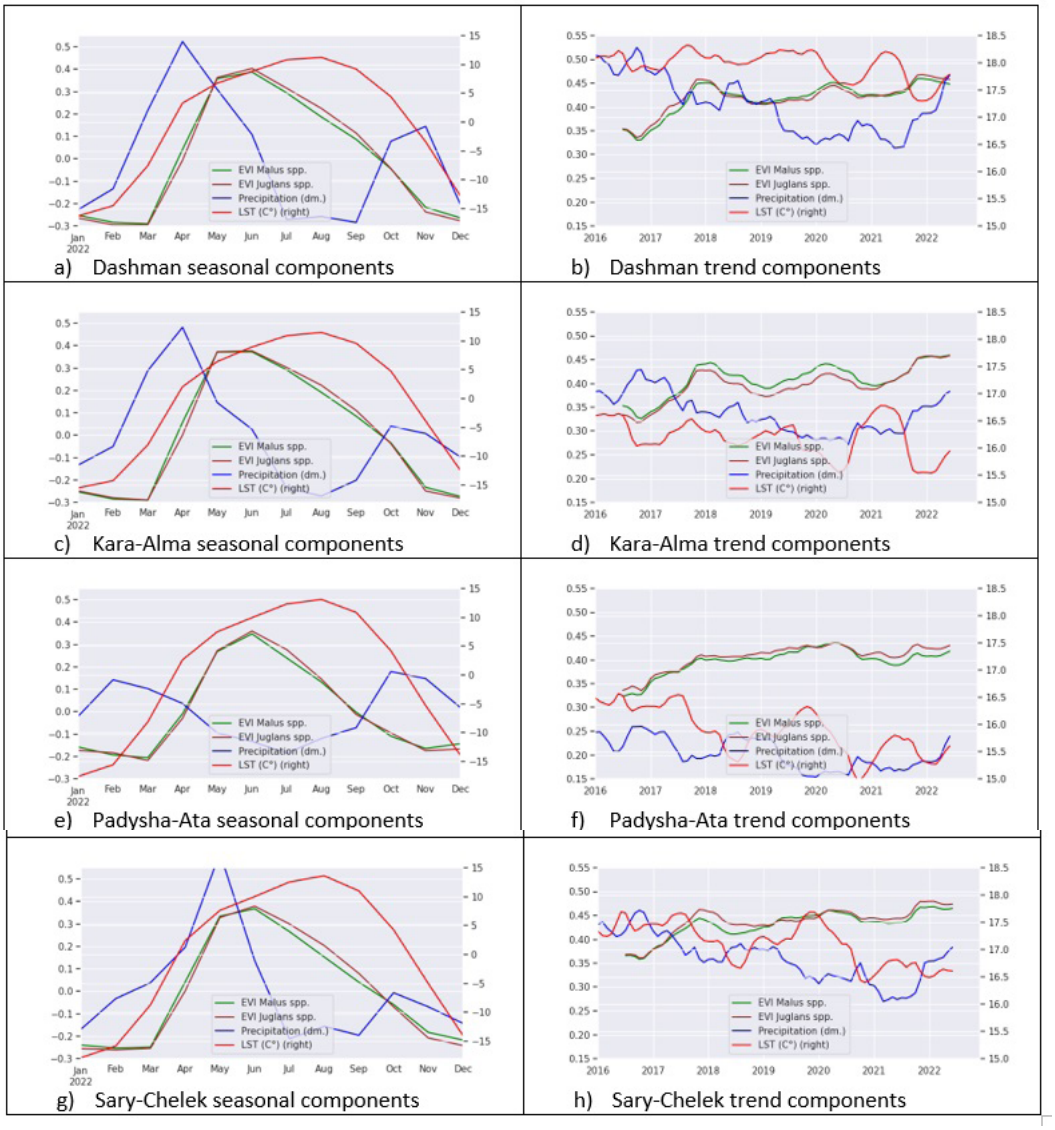

Figure 5. Seasonal and trend components of Malus spp. EVI (green), Juglans regia L. EVI (brown), precipitation (blue), and land surface temperature (red) with indication on the right vertical axis.

The seasonal distributions of EVI are similar among all the study sites and follow the phenological patterns of the vegetation, reaching their maxima in May-June after the peak of precipitation and before the peak of temperature (Figures 5a, c, e, g). The ascending and descending seasonal components of EVI of Malus spp. are more linear than those of Juglans regia L. (Figures 5a, c, e, g), especially in April and August to September.

3.4. Regression analysis

Two linear regression models were constructed for Malus spp. and Juglans regia L. with all tree data from all four study sites using Equation (5). The use of lags increased the coefficient of determination (R^2) from 0.61 to 0.731 for Malus spp.

and from 0.668 to 0.789 for Juglans regia L. (Tables II and III). Similarly, the use of thresholds to split the LST time series (using Equations 3 and 4) further increased the R2 to 0.755 for Malus spp. and 0.8 for Juglans regia L. (Tables II and III).

The lags of the best models were the same for both species except for the precipitation trend component, which was 5 months for Malus spp. and 2 months for Juglans regia L. (Tables II and III). The best thresholds for splitting the LST seasonal components were 9.7°C for Malus spp. and 10°C for Juglans regia L. The p-value for all the predictors exceeded the 0.01 significance level, indicating that all the predictors are significantly related to the response variable in the models (Tables II and III).

Table II. Malus spp. EVI regression

			R-squared: 0.755		Adj. R-squared: 0.755	
Precipitation trend	coef	std err	t	P>|t|	lag	hat threshold
Precipitation seasonal	-0.0014	8.2e-05	-16.710	0.000	5	NA
LST trend	0.0044	3.21e-05	13.192	0.000	2	NA
LST seasonal shoe	0.0045	0.000	136.823	0.000	12	NA
LST seasonal hat	0.0191	7.82e-05	244.035	0.000	0	9.7
const	-0.0276	0.001	-35.484	0.000	0	9.7
	0.4029	0.006	66.311	0.000	NA	NA

Table III. Juglans regia L. EVI regression

			R-squared: 0.800		Adj. R-squared: 0.800	
	coef	std err	t	P>|t|	lag	hat threshold
Precipitation trend	-0.0019	0.000	-18.770	0.000	2	NA
Precipitation seasonal	0.0046	0.000	19.572	0.000	2	NA
LST trend	0.0078	3.32e-05	138.378	0.000	12	NA
LST seasonal shoe	0.0200	7.92e-05	252.452	0.000	0	10
LST seasonal hat	-0.0245	0.001	-21.934	0.000	0	10
const	0.3593	0.007	50.507	0.000	NA	NA

The mean value of the LST trend component for Juglans regia L. was 16.7°C with a mean residual of 0.065°C, and for Malus spp. 16.8°C and 0.07°C, respectively. The mean trend values together with their respective "hat thresholds" (Tables II and III) show that LST values ≥ 26.7°C are suppressive temperatures for Juglans regia L. and ≥ 26.5°C are suppressive temperatures for Malus spp.

4. Discussion

The results indicate a similarity of walnut-fruit forests to typical Eurasian deciduous forests. However, understanding the phenology of the species facilitates the understanding of their response to climate change and seasonal redistribution of climatic parameters. Mountain areas have high spatial variability of abiotic factors such as solar radiation and precipitation, which leads to variability of environmental attributes such as soils and vegetation, and human influence due to rugged terrain. This is reflected in the different mean values of the LST and precipitation trend components (Figures 5b, d, f, h). Therefore, it is important to consider these factors in research and modeling of mountain ecosystems.

We chose EVI instead of NDVI to approximate forest vegetation phenology because it is an “optimized” vegetation index designed to enhance the vegetation signal from trees and increase sensitivity in high biomass regions, resulting in improved vegetation monitoring by separating the background signal from the canopy signal and reducing atmospheric effects (Landsat Enhanced Vegetation Index | U.S. Geological Survey, n.d.). EVI was also a better vegetation covariate for phenological studies conducted in North America using MODIS data (Peng et al., 2017). However, for land cover assessment in northeastern China, MODIS-NDVI showed better predictive power than MODIS-EVI (Li et al., 2010). New remotely sensed vegetation indices such as near infrared vegetation reflectance (NIRv) and solar induced chlorophyll fluorescence (SIF) have recently achieved better phenological approximations for deciduous forests than NDVI and EVI (Zhang et al., 2022). However, Cao et al. (2023) found EVI derived from Sentinel imagery to be one of the best covariates for phenology of mangrove forests in coastal areas of China.

While NDVI is very sensitive to chlorophyll, EVI is more sensitive to canopy structure, such as leaf area index (LAI), canopy type, and the overall appearance of the vegetation. EVI has been used extensively as a phenological covariate for various plant ecosystems (Peng et al., 2017). NDVI and EVI can complement each other in environmental studies, but since our focus was on phenology, we used EVI because it was specifically designed to better represent the tree canopy and is one of the most widely used indices with a long history of application.

The 10 m resolution of Sentinel imagery likely captures our large tree canopies within most of the area of a pixel. Thus, we expect most of the signal from a pixel

to come from the canopy. In addition, the large dataset of trees from different areas helps to reveal the signal characteristics of the species. In some plots, the forest was very homogeneous and dominated by one species, so the entire pixel could represent a signal from several canopies of the same species. However, when different tree species grew next to each other, the signal was contaminated by the contributions of other species. This is a limitation of this method, and it was not possible to discriminate the signal from different species in one pixel in our research.

The Ordinary Least Squares (OLS) linear regression model with extensive feature engineering such as trend and seasonal decomposition, time series splitting with a threshold, and lag shifts was chosen over more sophisticated machine learning approaches to develop a more understandable yet accurate model. The OLS linear model can clarify the relationships between variables and transformations, their significance, and helps to reveal the complexity of these relationships.

Both seasonal and trend components of precipitation showed a high predictive capacity for EVI. This is supported by many phenological studies in the region, but mainly working with grasslands and larger geographic scales (Gessner et al., 2013; Klein et al., 2012). The high predictive capacity of the seasonal components of climatic factors indicates that a substantial change in the amount or seasonal distribution of precipitation would have a major impact on the forests, especially on the Malus spp. and Juglans regia L. species (Tables II and III).

The seasonal component of LST is a promoting factor for vegetation in spring and EVI increases with temperature, whereas when temperature becomes very high in summer (LST around 26.5°C) it starts to suppress vegetation growth and EVI starts to decrease in July (Figures 5a, c, e, g). At the same time, decreasing precipitation in summer promotes increased stress for vegetation. We tried to capture this complexity by splitting the seasonal component of LST with a given threshold into two components, where the temperature below the threshold would be the promoting and the temperature above the threshold would be the suppressing vegetation growth. This resulted in an increase in R^2, as shown in the Results section. The negative effect of high temperature is also indicated by the fact that "LST seasonal hat" had negative coefficients in the regressions (Tables II and III). However, we believe that the decrease in the seasonal component of EVI after June (Figures 5a, c, e, g) is partly due to the annual phenological cycle. In practice, it is difficult to disentangle the effects of high temperature and cyclical leaf wilting. This complex behavior could be captured using a machine learning regression algorithm, but such a model would be difficult to interpret and would not reveal the underlying processes.

Our results show similar patterns of tree species seasonal phenology approximated by EVI in different study areas (Figures 5a, c, e, g). However, the absolute values of their trend components show different mean values (Figures 5b,

d, f, h). The main reason for this is the different elevation of the study sites (Figure 3c), as well as different LST and precipitation due to their high spatial heterogeneity attributed to mountainous conditions (Figures 5b, d, f, h). For example, Padysha-Ata is the highest of all study sites and thus has the lowest mean values of the LST and precipitation trend components (Figure 5f), and a different pattern of the seasonal precipitation component (Figure 5e, blue line). However, the values of the seasonal EVI component during winter are the highest among all study sites (Figure 5e, green and brown lines). This is most likely due to the lower level of precipitation resulting in less snow. This indicates that Padysha-Ata is different from the other three study sites in terms of environmental conditions. As a result, the mean value of the EVI trend component is also lower here than in the other three study sites (Figure 5f, green and brown lines). The soil types in all study sites are similar (Adyshev et al., 1987; Mamytov, 1974), so the difference in EVI is not due to different soil types, but also due to different landscape conditions.

The precipitation trend component had the highest predictive capacity at lag 5 (5 months) for Malus spp. and at lag 2 (2 months) for Juglans regia L., and it has a negative coefficient in the regression analysis ("precipitation trend" in Tables II and III). This is most likely due to the amount of snow. Intensive snowfall can have a negative impact on vegetation by delaying the onset of the growing season. We did not distinguish between solid and liquid precipitation, and the second precipitation peak of the seasonal component is in late fall and winter (Figures 5a, c, e, g); the seasonal precipitation component has a positive coefficient in the regression analysis output with a very close lag of 2 months for both species (Tables II and III). This also indicates a mixed effect of precipitation on vegetation and tree species, depending on the type of precipitation - snow or rain. It may be necessary to separate snow water from rain for more accurate modeling.

The seasonal distribution of precipitation is more important than its annual mean, as the "precipitation seasonal" coefficient has a larger absolute value than that of the "precipitation trend" (Tables II and III). On the other hand, the "LST trend component" had significant predictive power with a lag of 12 months, i.e., EVI responses to interannual temperature changes with a lag of one year (Tables II and III). This suggests that occasional high annual mean temperatures may have a positive effect by advancing the start of the growing season the following year. This hypothesis requires further research.

Temperature and precipitation have mixed effects on woody vegetation as approximated by EVI. For example, high winter snowfall can limit summer tree development, and high spring precipitation promotes tree development. Rapid warming in spring promotes tree development, while high summer temperatures suppress vegetation. However, a generally warmer year may advance the start of

the growing season in the following year. The resulting regression equation can be used to predict species behavior in response to changes or seasonal redistribution of the seasonal components of temperature and precipitation, as well as changes in the interannual mean of climatic factors. This approach helps to distinguish between seasonal and interannual changes and their effects.

The two different genera we studied (Malus spp. and Juglans regia L.) showed similar phenological behavior, but with significant differences between species and study sites. This is partly due to a mixed signal from understory vegetation and other trees. However, Malus spp. and Juglans regia L. showed a small but significant and consistent difference in the seasonal component of EVI across all four sites, as illustrated by higher EVI values of Malus spp. in April and higher EVI values of Juglans regia L. in June-September (Figures 5a, c, e, g). We found significant differences in EVI between species and sites during the growing season.

Our results shed light on the response of these tree species to climatic factors, and the regression analysis helps to model their behavior in response to climate change. Luo et al. (2019) predict more frequent precipitation and higher temperatures in the region. At the same time, Shaw et al. (2022) indicate that the phenological period of plants in Kyrgyzstan and Tajikistan will start 1-2 weeks earlier. All these factors will affect forest phenology and change the tree line. The overall gradual increase in the interannual mean temperature may have a positive effect on tree species by advancing the onset of the growing season and thus prolonging the growing season. However, the increase in summer heat will suppress tree growth and promote earlier senescence, forcing trees to seek cooler locations in the long term and shifting the tree line upwards. However, soils are thinner and have more coarse fragments at higher elevations, which may limit the vertical redistribution of species. However, as these species grow in the different conditions of elevation, LST and precipitation (Figures 3c, 5b, d, f, h), they show their adaptability within these ecological boundaries.

The redistribution of precipitation from solid to liquid may also benefit trees, as discussed above. However, in this case, some of the moisture provided by melting snow in the mountains may not be available in the future. Our research does not include water from streams, but some of it can be accounted for in the seasonal component of precipitation and the 2-month lag in the regression equation. The precipitation with a 2-month lag may partly be solid precipitation that becomes available after melting. Identifying the contribution of solid and liquid precipitation to vegetation development requires additional research. In principle, they can be separated, including their timing, but early and late winter precipitation can vary and be a significant source of error.

The results of this research demonstrate the high predictive power of the decomposed time series of climatic factors; however, fitting such models requires intensive field data collection and can be complicated, especially with respect to finding appropriate lags. However, modern computing capabilities allow the development of spatially explicit models with discrete modeling for each pixel. The results also indicate that even with such a relatively coarse resolution of satellite imagery, it is still possible to discriminate between species based on seasonal components of EVI. Our results could be further improved with more precise tree coordinates, finer spatial resolution of satellite imagery, and application of bias correction (Isaev, Kulikov, et al., 2022).

Limitations of the research include the coarse spatial resolution of satellite imagery, resulting in mixed signals from canopy and understory. The use of EVI can reduce the influence of the understory to some extent. The homogeneity of the forest also contributes to the clean signal from a given species, as one pixel may include several canopies, but they will mostly be of the same species. Accuracy of GPS coordinates is also an issue. However, since the forest is dominated by Juglans regia L. and Malus spp. is a minor component, this suggests that the signal from Juglans regia L. is cleaner than from Malus spp. These factors are very difficult to quantify and account for in this study. However, the consistency of results such as the seasonal component of EVI across study sites indicates the general accuracy of the results and the concept.

5. Conclusion

In this study, we used the remotely sensed vegetation index EVI derived from Sentinel imagery to determine the phenology of Juglans regia L. and Malus spp. trees in different parts of walnut-fruit forests in southern Kyrgyzstan and their relationship with climatic factors such as precipitation and land surface temperature. To do this, we decomposed the temperature and precipitation time series into trend and seasonal components and used them as predictors in an OLS linear regression for EVI time series for the different species. To increase the predictive capacity of the regression, we used intensive feature engineering such as temporal lags of the predictors and splitting the seasonal component of LST into two parts to account for the promoting effect of lower temperatures and the depressing effect of high temperatures on vegetation.

The results show the difference in phenology of the species approximated by the seasonal component of the EVI time series. This can be used to map tree species using sentinel time series. The overall approach of predicting EVI with the time series components of climatic factors shows its effectiveness, but extensive

feature engineering such as lagging and splitting the predictors with mixed effects needs to be employed. The overall approach is promising for predicting species behavior in a changing climate. Temperature and precipitation had mixed effects on vegetation, and to improve prediction it is crucial to distinguish between solid and liquid precipitation and between moderate and high temperatures.

In general, the seasonality of precipitation and temperature plays a greater role than the interannual means, as seasonal values have a greater predictive power for EVI. Seasonal redistribution of climatic parameters, even if their annual means do not change, will have a greater impact on vegetation than changes in annual means. Thus, more studies are needed to consider the seasonal phenology of vegetation and its relationship to climatic conditions.

Acknowledgement

Research was financially supported by the Critical Ecosystem Partnership Fund, project – "Conservation and Research of Wild Fruit Species in Western Tien Shan, Kyrgyz Republic" (CEPF-110679), authors declare no conflict of interests.

We would like to thank Samat Kalmuratov and Aiza Kuzovenko, whose help was invaluable during the field work. We would also like to thank the two anonymous reviewers, who generously provided their fair and helpful comments, which made a great contribution to the final product.

References

Adyshev, M. M., Kashirin, F. T., Umurzakov, S. U., Almaev, T. M., Voronina, A. F., Grigorenko, P. G., Dzhamgerchinov, B. D., Zabirov, R. D., Zinkova, Z. Y., Izmailov, A. E., Isabaeva, V. A., Kravchenko, A. V., Mamytov, A. M., Makhrina, L. I., Moldokulov, A. M., Murzaev, E. M., Otorbaev, K. O., Popova, L. I., Yar-Mukhamedov, G. K., … Chernova, L. I. (1987). *Atlas Kirgizskoj SSR* [Atlas of the Kyrgyz SSR (vol. I)] (in Russian). Fabrika#4.

Aitaliev, A. M., Sakyev, D. D., Nazarkulov, K. B., Amanova, M. T., Berezhneva, V. A., Spektorenko, N. B., Aidaraliev, N. A., Sataev, S. A., Jumanazarova, A. J., Ymanbekov, K. Y., Usupashev, S. E., & Nurdinov, A. N. (2020). *Atlas of natural and man-made hazards on the territory of the Kyrgyz Republic* (in Russian). Department of Monitoring and Forecasting of Emergency Situations of the Ministry of Emergency Situations of the Kyrgyz Republic.

Azarov, A., Polesny, Z., Darr, D., Kulikov, M., Verner, V., & Sidle, R. C. (2022). Classification of Mountain Silvopastoral Farming Systems in Walnut Forests of Kyrgyzstan: Determining Opportunities for Sustainable Livelihoods. *Agriculture*, 12(12), 2004. https://doi.org/10.3390/AGRICULTURE12122004

Beer, R., Kaiser, F., Schmidt, K., Ammann, B., Carraro, G., Grisa, E., & Tinner, W. (2008). Vegetation history of the walnut forests in Kyrgyzstan (Central Asia): natural or anthropogenic origin? *Quaternary Science Reviews*, 27(5–6), 621–632. https://doi.org/10.1016/j.quascirev.2007.11.012

Beer, R., & Tinner, W. (2008). Four thousand years of vegetation and fire history in the spruce forests of northern Kyrgyzstan (Kungey Alatau, Central Asia). *Vegetation History and Archaeobotany,* 17(6), 629–638. https://doi.org/10.1007/s00334-008-0142-1

Beer, R., Tinner, W., Carraro, G., & Grisa, E. (2007). Pollen representation in surface samples of the Juniperus, Picea and Juglans forest belts of Kyrgyzstan, central Asia. *The Holocene*, 17(5), 599–611. https://doi.org/10.1177/0959683607078984

Borchardt, P., Oldeland, J., Ponsens, J., & Schickhoff, U. (2013). Plant functional traits match grazing gradient and vegetation patterns on mountain pastures in SW Kyrgyzstan. *Phytocoenologia,* 43(3), 171–181. https://doi.org/10.1127/0340-269X/2013/0043-0542

Borchardt, P., Schmidt, M., & Schickhoff, U. (2010). Vegetation patterns in Kyrgyzstan's walnut-fruit forests under the impact of changing forest use in post-soviet transformation. *Erde*, 141(3), 255–275.

Botschantzeva, Z. P., & Varekamp, H. Q. (1982). Tulips : taxonomy, morphology, cytology, phytogeography and physiology. Balkema.

Cantarello, E., Lovegrove, A., Orozumbekov, A., Birch, J., Brouwers, N., & Newton, A. C. (2014). Human Impacts on Forest Biodiversity in Protected Walnut-Fruit Forests in Kyrgyzstan. *Journal of Sustainable Forestry*, 33(5), 454–481. https://doi.org/10.1080/10549811.2014.901918

Cao, J., Xu, X., Zhuo, L., & Liu, K. (2023). Investigating mangrove canopy phenology in coastal areas of China using time series Sentinel-1/2 images. *Ecological Indicators*, 154, 110815. https://doi.org/10.1016/J.ECOLIND.2023.110815

Cornille, A., Giraud, T., Smulders, M. J. M., Roldán-Ruiz, I., & Gladieux, P. (2014). The domestication and evolutionary ecology of apples. *Trends in Genetics*, 30(2), 57–65. https://doi.org/10.1016/j.tig.2013.10.002

Dai, X., Yang, G., Liu, D., & Wan, R. (2020). Vegetation Carbon Sequestration Mapping in Herbaceous Wetlands by Using a MODIS EVI Time-Series Data Set: A Case in Poyang Lake Wetland, China. *Remote Sensing*, 12(18), 3000. https://doi.org/10.3390/RS12183000

Dulamsuren, C., Khishigjargal, M., Leuschner, C., & Hauck, M. (2014). Response of tree-ring width to climate warming and selective logging in larch forests of the Mongolian Altai. *Journal of Plant Ecology*, 7(1), 24–38. https://doi.org/10.1093/JPE/RTT019

Dulamsuren, C., Wommelsdorf, T., Zhao, F., Xue, Y., Zhumadilov, B. Z., Leuschner, C., & Hauck, M. (2013). Increased Summer Temperatures Reduce the Growth and Regeneration of Larix sibirica in Southern Boreal Forests of Eastern Kazakhstan. *Ecosystems*, 16(8), 1536–1549. https://doi.org/10.1007/s10021- 013-9700-1

Eckert, S. (2012). Improved Forest Biomass and Carbon Estimations Using Texture Measures from WorldView-2 Satellite Data. *Remote Sensing*, 4(4), 810–829. https://doi.org/10.3390/RS4040810

Fang, X., Chen, Z., Guo, X., Zhu, S., Liu, T., Li, C., & He, B. (2019). Impacts and uncertainties of climate/CO2 change on net primary productivity in Xinjiang, China (2000–2014): A modelling approach. *Ecological Modelling*, 408. https://doi.org/10.1016/j.ecolmodel.2019.108742

Gao, X., Huete, A. R., Ni, W., & Miura, T. (2000). Optical-Biophysical Relationships of Vegetation Spectra without Background Contamination. *Remote Sensing of Environment*, 74(3), 609–620. https://doi.org/10.1016/S0034-4257(00)00150-4

Gessner, U., Naeimi, V., Klein, I., Kuenzer, C., Klein, D., & Dech, S. (2013). The relationship between precipitation anomalies and satellite-derived vegetation activity in Central Asia. *Global and Planetary Change*, 110(0), 74–87. https://doi.org/10.1016/j.gloplacha.2012.09.007

Henebry, G., Tomaszewska, M., & Kelgenbaeva, K. (2017). Linkages between Snow Cover Seasonality, Terrain, and Land Surface Phenology in the Highland Pastures of Kyrgyzstan. I*n Geophysical Research Abstracts* (Vol. 19).

Huete, A., Didan, K., Miura, T., Rodriguez, E. P., Gao, X., & Ferreira, L. G. (2002). Overview of the radiometric and biophysical performance of the MODIS vegetation indices. *Remote Sensing of Environment*, 83(1–2), 195–213. https://doi.org/10.1016/S0034-4257(02)00096-2

Isaev, E., Ermanova, M., Sidle, R. C., Zaginaev, V., Kulikov, M., & Chontoev, D. (2022). Reconstruction of Hydrometeorological Data Using Dendrochronology and Machine Learning Approaches to Bias-Correct Climate Models in Northern Tien Shan, Kyrgyzstan. *Water*, 14(15), 2297. https://doi.org/10.3390/W14152297

Isaev, E., Kulikov, M., Shibkov, E., & Sidle, R. C. (2022). Bias correction of Sentinel-2 with unmanned aerial vehicle multispectral data for use in monitoring walnut-fruit forest in western Tien Shan, Kyrgyzstan. *Journal of Applied Remote Sensing*, 17(2), 022204. https://doi.org/10.1117/1.JRS.17.022204

IUCN. (2022). The IUCN Red List of Threatened Species. *Version 2022-2*. https://www.iucnredlist.org

IUSS Working Group WRB. (2006). World reference base for soil resources 2006. *In World Soil Resources Reports* No. 103 (Vol. 43, Issue 02). https://doi.org/10.1017/S0014479706394902

Jiang, F., Kutia, M., Ma, K., Chen, S., Long, J., & Sun, H. (2021). Estimating the aboveground biomass of coniferous forest in Northeast China using spectral variables, land surface temperature and soil moisture. *Science of The Total Environment*, 785, 147335. https://doi.org/10.1016/J.SCITOTENV.2021.147335

Kang, J., Shishov, V. V., Tychkov, I., Zhou, P., Jiang, S., Ilyin, V. A., Ding, X., & Huang, J. G. (2022). Response of model-based cambium phenology and climatic factors to tree growth in the Altai Mountains, Central Asia. *Ecological Indicators*, 143, 109393. https://doi.org/10.1016/J.ECOLIND.2022.109393

Kariyeva, J., Leeuwen, W. J. D. van, & Woodhouse, C. A. (2012). Impacts of climate gradients on the vegetation phenology of major land use types in Central Asia (1981-2008). *Frontiers of Earth Science*, 6(2), 206–225. https://doi.org/10.1007/S11707-012-0315-1

Klein, I., Gessner, U., & Kuenzer, C. (2012). Regional land cover mapping and change detection in Central Asia using MODIS time-series. *Applied Geography*, 35(1–2), 219–234. https://doi.org/Doi 10.1016/J.Apgeog.2012.06.016

Kulikov, M., & Schickhoff, U. (2017). Vegetation and climate interaction patterns in Kyrgyzstan: spatial discretization based on time series analysis. *Erdkunde*, 71(2), 143–165. https://doi.org/10.3112/erdkunde.2017.02.04

Kulikov, M., Schickhoff, U., Gröngröft, A., & Borchardt, P. (2017). Modelling Soil Erodibility in Mountain Rangelands of South-Western Kyrgyzstan. *Pedosphere*. https://doi.org/10.1016/S1002-0160(17)60402-8

Landsat Enhanced Vegetation Index | U.S. Geological Survey. (n.d.). Retrieved September 13, 2022, from https://www.usgs.gov/landsat-missions/landsat-enhanced-vegetation-index

Lazkov, G. A., & Sultanova, B. A. (2011). Checklist of vascular plants of Kyrgyzstan (A. N. Sennikov (Ed.)). Botanical Museum, Finnish Museum of Natural History, University of Helsinki.

Li, C., Wang, R., Cui, X., Wu, F., Yan, Y., Peng, Q., Qian, Z., & Xu, Y. (2021). Responses of vegetation spring phenology to climatic factors in Xinjiang, China. *Ecological Indicators*, 124, 107286. https://doi.org/10.1016/J.ECOLIND.2020.107286

Li, C., Zhang, C., Luo, G., & Chen, X. (2013). Modeling the carbon dynamics of the dryland ecosystems in Xinjiang, China from 1981 to 2007—The spatiotemporal patterns and climate controls. *Ecological Modelling*, 267, 148–157. https://doi.org/10.1016/J.ECOLMODEL.2013.06.007

Li, Z., Li, X., Wei, D., Xu, X., & Wang, H. (2010). An assessment of correlation on MODIS-NDVI and EVI with natural vegetation coverage in Northern Hebei Province, China. *Procedia Environmental Sciences*, 2, 964–969. https://doi.org/10.1016/j.proenv.2010.10.108

Loranty, M. M., Davydov, S. P., Kropp, H., Alexander, H. D., Mack, M. C., Natali, S. M., & Zimov, N. S. (2018). Vegetation Indices Do Not Capture Forest Cover Variation in Upland Siberian Larch Forests. *Remote Sensing*, 10(11), 1686. https://doi.org/10.3390/RS10111686

Luo, M., Liu, T., Meng, F., Duan, Y., Bao, A., Xing, W., Feng, X., De Maeyer, P., & Frankl, A. (2019). Identifying climate change impacts on water resources in Xinjiang, China. *Science of The Total Environment*, 676, 613–626. https://doi.org/10.1016/J.SCITOTENV.2019.04.297

Mace, G. M. (2004). The role of taxonomy in species conservation. Philosophical Transactions of the Royal Society of London. *Series B: Biological Sciences*, 359(1444), 711–719. https://doi.org/10.1098/RSTB.2003.1454

Mamytov, A. M. (1974). Soils of Kyrgyz SSR (in Russian). Ilim.

Molnar, T. (2011). Persian Walnuts (Juglans regia L.) in Central Asia. *Annual Report of the Northern Nut Growers Association*, 101, 56–69.

Orozumbekov, A., Cantarello, E., & Newton, A. C. (2014). Status, distribution and use of threatened tree species in the walnut-fruit forests of Kyrgyzstan. Forests, *Trees and Livelihoods*, 24(1), 1–17. https://doi.org/10.1080/14728028.2014.928604

Peng, D., Wu, C., Li, C., Zhang, X., Liu, Z., Ye, H., Luo, S., Liu, X., Hu, Y., & Fang, B. (2017). Spring green-up phenology products derived from MODIS NDVI and EVI: Intercomparison, interpretation and validation using National Phenology Network and AmeriFlux observations. *Ecological Indicators*, 77, 323–336. https://doi.org/10.1016/j.ecolind.2017.02.024

Propastin, P. A., Kappas, M., Erasmi, S., & Muratova, N. R. (2007). Remote sensing based study on intra-annual dynamics of vegetation and climate in drylands of Kazakhstan. *Basic and Applied Dryland Research*, 1(2), 138–154. https://doi.org/10.1127/badr/1/2007/138

Propastin, P. A., Kappas, M., & Muratova, N. R. (2008a). A remote sensing based monitoring system for discrimination between climate and human-induced vegetation change in Central Asia. *Management of Environmental Quality: An International Journal*, 19(5), 579–596. https://doi.org/http://dx.doi.org/10.1108/14777830810894256

Propastin, P. A., Kappas, M., & Muratova, N. R. (2008b). Inter-annual changes in vegetation activities and their relationship to temperature and precipitation in Central Asia from 1982 to 2003. *Journal of Environmental Informatics*, 12(2), 75–87. https://doi.org/10.3808/jei.200800126

Rahman, A. F., Sims, D. A., Cordova, V. D., & El-Masri, B. Z. (2005). Potential of MODIS EVI and surface temperature for directly estimating per-pixel ecosystem C fluxes. *Geophysical Research Letters*, 32(19), 1–4. https://doi.org/10.1029/2005GL024127

SAEPF, IBP-NAS-KR, & Aleine. (2006). Kyrgyz Republic Red Data Book (A. Davletkeldiev, E. Shukurov, A. Chynkojoev, A. Burhanov, S. Mamatov, T. Musuraliev, S. Asylbaeva, R. Ionov, E. Kasybekov, I. Soodanbekov, V. Surappaeva, E. Turdukulov, & U. Mambetaliev (Eds.); 2nd ed.). FAO NFPF.

Schickhoff, U., Bobrowski, M., Böhner, J., Bürzle, B., Chaudhary, R. P., Gerlitz, L., Heyken, H., Lange, J., Müller, M., Scholten, T., Schwab, N., & Wedegärtner, R. (2015). Do Himalayan treelines respond to recent climate change? An evaluation of sensitivity indicators. *Earth System Dynamics*, 6(1), 245–265. https://doi.org/10.5194/ESD-6-245-2015

Shaw, R., Luo, Y., Cheong, T. S., Halim, S. A., Chaturvedi, S., Hashizume, M., Insarov, G. E., Ishikawa, Y., Jafari, M., Kitoh, A., Pulhin, J., Singh, C., Vasant, K., & Zhang, Z. (2022). Asia. In: Climate Change 2022: Impacts, Adaptation and Vulnerability. *Contribution of Working Group II to the Sixth Assessment Report of the Intergovernmental Panel on Climate Change*. https://doi.org/10.1017/9781009325844.012

Shigaeva, J., Dzhakypbekova, K., Nurdoolot Kyzy, C., Darr, D., & Wolff, H.-P. (2018). Profitability of forest products of walnut-fruit forest of Kyrgyzstan vs agricultural production, case study from Kyzyl Unkur villages. World Mountain Forum.

Shigaeva, J., Kollmair, M., Niederer, P., & Maselli, D. (2007). Livelihoods in transition: changing land use strategies and ecological implications in a post-Soviet setting (Kyrgyzstan). *Central Asian Survey*, 26(3), 389–406. https://doi.org/10.1080/02634930701702696

Spengler, R. N. (2019). Origins of the apple: The role of megafaunal mutualism in the domestication of Malus and rosaceous trees. *Frontiers in Plant Science*, 10, 617. https://doi.org/10.3389/FPLS.2019.00617/BIBTEX

statsmodels.regression.linear_model.OLS - statsmodels 0.15.0 (+59). (n.d.). Retrieved September 21, 2023, from https://www.statsmodels.org/dev/generated/statsmodels.regression.linear_model.OLS.html

statsmodels.stats.weightstats.ttest_ind - statsmodels 0.14.0. (n.d.). Retrieved September 19, 2023, from https://www.statsmodels.org/stable/generated/statsmodels.stats.weightstats.ttest_ind.html

statsmodels.tsa.seasonal.seasonal_decompose — statsmodels (0.14.0). (2023). https://www.statsmodels.org/dev/generated/statsmodels.tsa.seasonal.seasonal_decompose.html

Tomaszewska, M. A., & Henebry, G. M. (2020). How much variation in land surface phenology can climate oscillation modes explain at the scale of mountain pastures in Kyrgyzstan? International *Journal of Applied Earth Observation and Geoinformation*, 87, 102053. https://doi.org/10.1016/j.jag.2020.102053

Tomaszewska, M. A., Nguyen, L. H., & Henebry, G. M. (2020). Land surface phenology in the highland pastures of montane Central Asia: Interactions with snow cover seasonality and terrain characteristics. *Remote Sensing of Environment*, 240, 111675. https://doi.org/10.1016/j.rse.2020.111675

Torokeldiev, N., Ziehe, M., Gailing, O., & Finkeldey, R. (2019). Genetic diversity and structure of natural Juglans regia L. populations in the southern Kyrgyz Republic revealed by nuclear SSR and EST-SSR markers. *Tree Genetics and Genomes*, 15(1), 1–12. https://doi.org/10.1007/s11295-018-1311-8

User Guides - Sentinel-2 MSI - Sentinel Online - Sentinel Online. (2023). https://sentinels.copernicus.eu/web/sentinel/user-guides/sentinel-2-msi

van Nocker, S., Berry, G., Najdowski, J., Michelutti, R., Luffman, M., Forsline, P., Alsmairat, N., Beaudry, R., Nair, M. G., & Ordidge, M. (2012). Genetic diversity of red-fleshed apples (Malus). *Euphytica*, 185(2), 281–293. https://doi.org/10.1007/s10681-011-0579-7

Vinceti, B., Elias, M., Azimov, R., Turdieva, M., Aaliev, S., Bobokalonov, F., Butkov, E., Kaparova, E., Mukhsimov, N., Shamuradova, S., Turgunbaev, K., Azizova, N., & Loo, J. (2022). Home gardens of Central Asia: Reservoirs of diversity of fruit and nut tree species. *PLOS ONE*, 17(7), e0271398. https://doi.org/10.1371/JOURNAL.PONE.0271398

Volk, G. M., Henk, A. D., Richards, C. M., Forsline, P. L., & Thomas Chao, C. (2013). Malus sieversii: A diverse central asian apple species in the USDA-ARS national plant germplasm system. *HortScience*, 48(12), 1440–1444.

Wang, X., Li, C., Liang, D., Zou, Y., Li, P., & Ma, F. (2015). Phenolic compounds and antioxidant activity in red-fleshed apples. *Journal of Functional Foods*, 18, 1086–1094. https://doi.org/10.1016/j.jff.2014.06.013

Wang, Y., Sylvester, S. P., Lu, X., Dawadi, B., Sigdel, S. R., Liang, E., & Julio Camarero, J. (2019). The stability of spruce treelines on the eastern Tibetan Plateau over the last century is explained by pastoral disturbance. *Forest Ecology and Management*, 442, 34–45. https://doi.org/10.1016/J.FORECO.2019.03.058

Wilson, B., Dolotbakov, A., Burgess, B. J., Clubbe, C., Lazkov, G., Shalpykov, K., Ganybaeva, M., Sultangaziev, O., & Brockington, S. F. (2021). Central Asian wild tulip conservation requires a regional approach, especially in the face of climate change. *Biodiversity and Conservation*, 1–26. https://doi.org/10.1007/s10531-021-02165-z

Wilson, B., Mills, M., Kulikov, M., & Clubbe, C. (2019). The future of walnut-fruit forests in Kyrgyzstan and the status of the iconic Endangered apple Malus niedzwetzkyana. *Oryx*, 1–9. https://doi.org/10.1017/S0030605318001230

Winter, M. B., Wolff, B., Gottschling, H., & Cherubini, P. (2009). The impact of climate on radial growth and nut production of Persian walnut (Juglans regia L.) in South Kyrgyzstan. *European Journal of Forest Research*, 128(6), 531–542. https://doi.org/10.1007/s10342-009-0295-1

Wu, L., Zhao, C., Li, J., Yan, Y., Han, Q., Li, C., & Zhu, J. (2023). Impact of extreme climates on land surface phenology in Central Asia. *Ecological Indicators*, 146. https://doi.org/10.1016/J.ECOLIND.2022.109832

Xiao, J., Chevallier, F., Gomez, C., Guanter, L., Hicke, J. A., Huete, A. R., Ichii, K., Ni, W., Pang, Y., Rahman, A. F., Sun, G., Yuan, W., Zhang, L., & Zhang, X. (2019). Remote sensing of the terrestrial carbon cycle: A review of advances over 50 years. *Remote Sensing of Environment*, 233. https://doi.org/10.1016/J.RSE.2019.111383

Yan, G., Long, H., Song, W., & Chen, R. (2008). Genetic polymorphism of Malus sieversii populations in Xinjiang, China. *Genetic Resources and Crop Evolution*, 55(1), 171–181. https://doi.org/10.1007/s10722-007-9226-5

Zaginaev, V., Ballesteros-Cánovas, J. A., Erokhin, S., Matov, E., Petrakov, D., & Stoffel, M. (2016). Reconstruction of glacial lake outburst floods in northern Tien Shan: Implications for hazard assessment. *Geomorphology*, 269, 75–84. https://doi.org/10.1016/J.GEOMORPH.2016.06.028

Zaginaev, V., Petrakov, D., Erokhin, S., Meleshko, A., Stoffel, M., & Ballesteros-Cánovas, J. A. (2019). Geomorphic control on regional glacier lake outburst flood and debris flow activity over northern Tien Shan. *Global and Planetary Change*, 176, 50–59. https://doi.org/10.1016/J.GLOPLACHA.2019.03.003

Zhang, C., Lu, D., Chen, X., Zhang, Y., Maisupova, B., & Tao, Y. (2016). The spatiotemporal patterns of vegetation coverage and biomass of the temperate deserts in Central Asia and their relationships with climate controls. *Remote Sensing of Environment*, 175, 271–281. https://doi.org/10.1016/j.rse.2016.01.002

Zhang, J., Xiao, J., Tong, X., Zhang, J., Meng, P., Li, J., Liu, P., & Yu, P. (2022). NIRv and SIF better estimate phenology than NDVI and EVI: Effects of spring and autumn phenology on ecosystem production of planted forests. *Agricultural and Forest Meteorology*, 315. https://doi.org/10.1016/J.AGRFORMET.2022.108819

Zhu, S., Li, C., Shao, H., Ju, W., & Lv, N. (2019). The response of carbon stocks of drylands in Central Asia to changes of CO2 and climate during past 35 years. *Science of The Total Environment*, 687, 330–340. https://doi.org/10.1016/J.SCITOTENV.2019.06.089

Zonneveld, B. J. M. (2009). The systematic value of nuclear genome size for “all” species of Tulipa L. (Liliaceae). P*lant Systematics and Evolution*, 281(1–4), 217–245. https://doi.org/10.1007/s00606-009-0203-7